Radiography and Arthrography

S. G. Davies

Contents

Abstract

The main emphasis of this chapter is a description of basic radiography of the wrist and hand with detailed description of radiographic technique and evaluation of the different projections. Static and dynamic carpal instability evaluation is vital for the assessment of ligamentous disruption. These techniques are covered in this chapter. There are a whole variety of measurement techniques which can be used in the assessment of wrist pathology. Following distal radial fracture, radial inclination, radial length and palmar tilt are important. Ulna variance is also assessed following distal radial fracture and in the context of ulnar-sided wrist pain. The scapholunate angle and capitate lunate angle are assessed when intercalated instability is suspected. Finally, the carpal height is a measurement which is applied when there is evidence of carpal collapse or loss of joint space. Arthrography still has a place in the modern assessment of the wrist. Radiocarpal and to a lesser extent midcarpal injection techniques may be employed.

1 Introduction

Plain film radiography has a fundamental role in the evaluation of the hand and wrist following trauma, in cases of suspected arthropathy, as part of an evaluation for certain systemic disorders with hand manifestations and in other miscellaneous situations such as tumour masses and pain.

S. G. Davies (✉)
Consultant Radiologist, Radiology Department, Royal Glamorgan Hospital, Rhondda Cynon Taf, Llantrisant, CF72 8XR, UK
e-mail: Stephen.Davies1@wales.nhs.uk

A. M. Davis et al. (eds.), *Imaging of the Hand and Wrist*, Medical Radiology. Diagnostic Imaging,
DOI: 10.1007/174_2010_136,

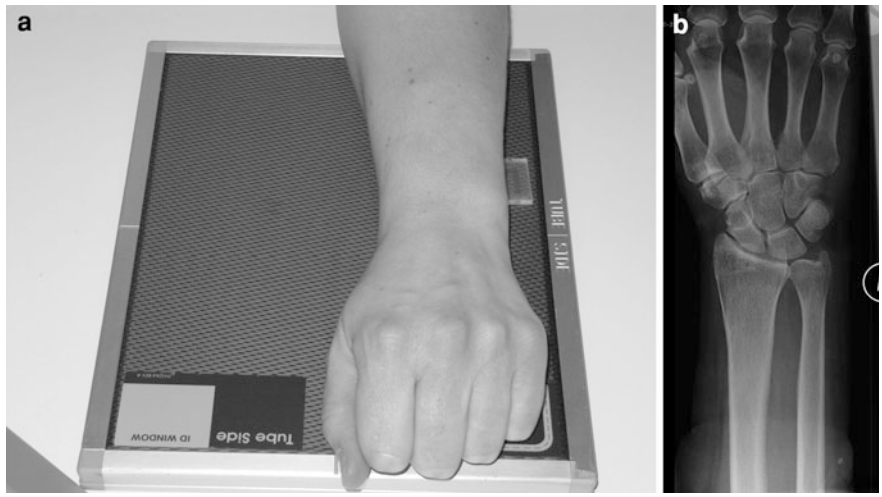

Fig. 1 **a** Patient positioning for posteroanterior (PA) wrist radiograph. **b** PA radiograph of wrist

2 Radiographic Projections

2.1 Radiographic Projections of the Wrist

The standard wrist projections are postero-anterior (PA) and lateral (Whitley 2005). Occasionally an oblique projection is added.

2.1.1 PA and Lateral Projections of the Wrist

Technique

The PA projection is performed with the patient seated. The shoulder is 90° abducted and the elbow is 90° flexed. The forearm is held in a neutral position with the hand flat on the table top. The tabletop should be at the same height as the forearm. The centering point is midway between the radial and ulnar styloid. The field of projection should include the distal half of the radius and ulna extending distantly to include the proximal two-thirds of the metacarpals (Fig. 1).

There are two different methods for obtaining the lateral projection of the wrist. The simplest method is to rotate the hand 90° maintaining the elbow in a flexed position. With this method, the ulna stays in a fixed position and the radius rotates through 90° along with the carpus. The second method involves rotation of both ulna and radius through 90°. This is achieved by extending the elbow and rotating the humerus through 90°. This latter method has the benefit of enabling a second projection at 90° to the first of the ulna. The centering point for both methods is the radial styloid (Fig. 2).

Evaluation

The PA projection of the wrist is useful in the evaluation of injuries to the distal radius and ulna, carpus and proximal metacarpals. It is also helpful in the evaluation of pathology such as erosions to the distal radius and ulna and carpus. The PA wrist should profile the extensor carpi ulnaris tendon groove which should be at the level of, or radial to the base of the ulnar styloid (Fig. 1) (Goldfarb and Yin 2001).

The positioning of the lateral projection of the wrist is evaluated with reference to the palmar cortex of the pisiform (Yang and Mann 1997). A well-positioned and centered lateral projection results in the palmar cortex of the pisiform lying between the palmar cortices of the distal scaphoid and capitate (Fig. 2).

The PA view of the wrist displays the carpal anatomy (Fig. 3). The carpal bones are arranged in proximal and distal rows. The proximal row comprises the scaphoid, lunate and triquetral, whilst the distal row is made up of the trapezium, trapezoid, capitate and hamate. The normal anatomic relationships of the wrist should demonstrate parallel opposing articular surfaces with symmetrical width of all intercarpal joints (Resnik 2000). The articular surfaces of the carpal bones should be normally aligned in three arcs (Fig. 4) (Gilula 1979). Arc I describes the outer proximal convexities of

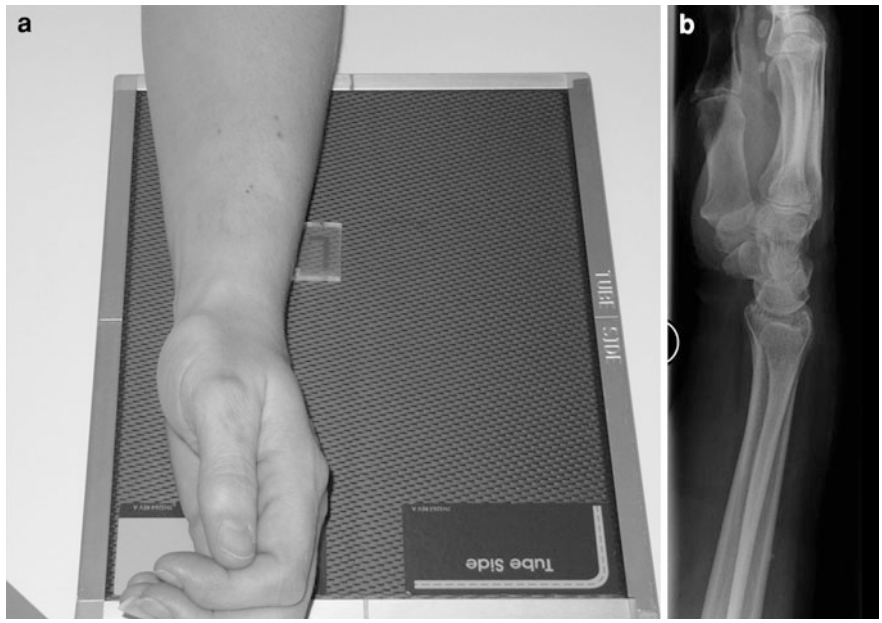

Fig. 2 **a** Patient positioning for lateral wrist radiograph. **b** Lateral radiograph of wrist

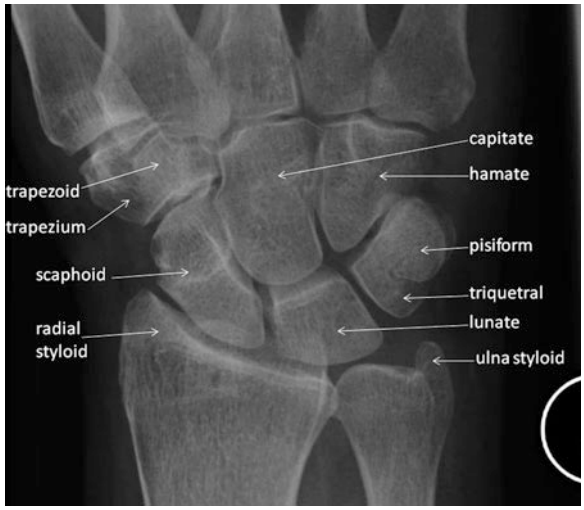

Fig. 3 Carpal anatomy

Fig. 4 Carpal arcs

scaphoid, lunate and triquetrum. Arc II describes the distal concavities of the scaphoid lunate and triquetrum. Arc III describes the proximal convexities of the capitate and lunate. For optimal demonstration, the wrist must be imaged PA in the neutral position. Two normal anatomical variants of the arcs are recognized (Loredo and Sorge 2005). The first variant is that the triquetrum may be shorter in its proximal–distal dimension than the adjacent lunate. This gives rise to discontinuity of arc I. The second variant is that the proximal hamate may be unusually prominent and rounded thereby creating discontinuity of arc III. Evaluation of the integrity of the arcs is important when assessing for fractures, dislocations and instability.

An important feature of the lateral wrist is the alignment of the radius, lunate and capitate (Fig. 5). These structures should be within 10° of coaxial alignment (Gilula 1979). It is noted that they are truly co-axial in only 11% of cases.

Fig. 5 Lateral wrist demonstrating axis for lateral alignment (not co-axial in this case)

2.2 Radiographic Projections of the Scaphoid Carpus

There are four standard projections for radiography of the scaphoid. They are the AP with ulnar deviation (plus or minus tube angulation), anterior oblique (pronated oblique), posterior oblique (supinated oblique) and lateral. This series is designed to provide tangential projections of the carpal bones with particular emphasis on evaluation of the scaphoid. The prime indication for these projections is the presence of trauma to the carpus particularly if there is associated tenderness in the region of the scaphoid.

2.2.1 AP with Ulnar Deviation

Technique

The patient sits to the side of the table with a flexed elbow and pronated forearm. The elbow and wrist are at the level of the tabletop. The hand is deviated in the ulnar direction (Fig. 6). The purpose of the deviation is to reduce the foreshortening of the scaphoid seen on the standard PA projection. When the wrist is in the normal neutral position the scaphoid is tilted (Gilula 1979). Additionally, the X-ray tube may be angled towards the elbow by 20° (Fig. 7) which further compensates for the normal scaphoid tilt.

The centering point is midway between the ulna and radial styloid processes. The film should include the distal radius and ulna and proximal metacarpals.

Evaluation

The PA projection should produce a good projection of the length of the scaphoid aiming at visualisation of clear joint space around the whole of the scaphoid (Fig. 6). Occasionally, there is some distal overlap. The radial styloid and ulnar styloid should be clearly seen.

2.2.2 Anterior Oblique (Pronated Oblique)

Technique

The wrist is externally rotated from the PA neutral position by 45° (Fig. 8). The radial styloid is, therefore, elevated from the tabletop. The centering point is midway between the ulnar and radial styloid. The fingers may be slightly flexed with the thumb held in front.

Evaluation

This projection (Fig. 8) gives a good demonstration of the distal scaphoid and trapezium. It is also a useful projection for evaluating the trapezoid and bases of the first and second metacarpals. The radial styloid and dorsal surface of the triquetrum is visible. Consideration may be given to applying a degree of ulnar deviation to this projection for better visualisation of the scaphoid.

2.2.3 Posterior Oblique (Supinated Oblique)

Technique

From the anterior oblique the wrist is externally rotated a further 90° (Fig. 9). The fingers are held together. The centering point is the ulnar styloid.

Evaluation

This projection demonstrates the pisiform and the piso-triquetral joint (Fig. 9). It is also useful for evaluating the hook of the hamate and bases of the fourth and fifth metacarpals. The long axis of the scaphoid lies perpendicular to the cassette.

2.2.4 Lateral

Technique

The technique is as described for the standard lateral view of the wrist (Sect. 2.1). However, a narrower field of view is generally used including only the

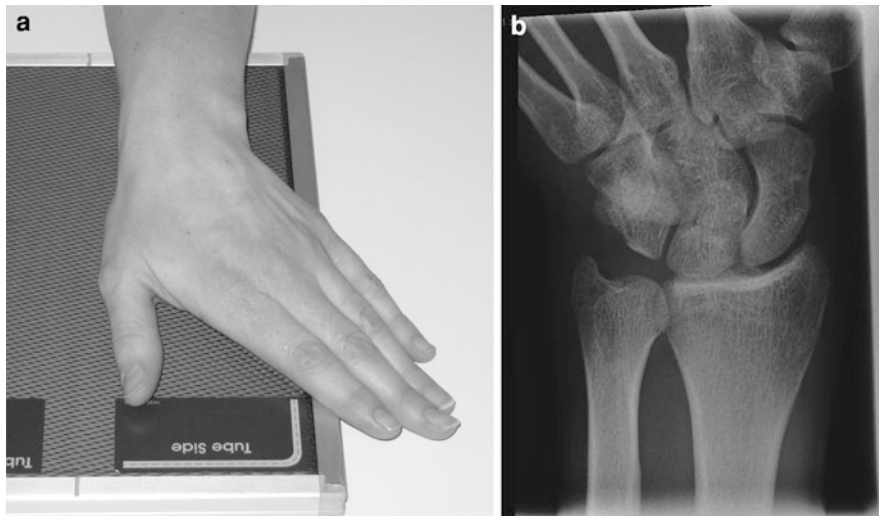

Fig. 6 **a** Patient positioning for AP carpus with ulna deviation. **b** AP radiograph with ulna deviation of carpus

Fig. 7 AP radiograph with ulna deviation and 20° of tube angulation

distal aspect of the radius and ulna and proximal metacarpal bases (Fig. 10).

Evaluation

The lateral projection is particularly valuable in assessing the dorsal surface of distal radius for fracture. This projection enables an evaluation of the alignment of the distal radius, lunate and capitate (Fig. 10). This projection is useful when assessing for dislocation and carpal instability.

2.3 Radiographic Projections of the Hand

There are two standard projections for the hand which are the PA and anterior oblique projections. Supplementary projections include the lateral projection and the posterior oblique projection.

2.3.1 PA Hand

Technique

The forearm is pronated and the hand rests on the cassette (Fig. 11). The ulnar styloid and radial styloid should lie equidistant from the tabletop. The centering point is the third metacarpal head. This projection should include the whole of the fingers (phalanges), metacarpals, carpus together with distal ends of the radius and ulna.

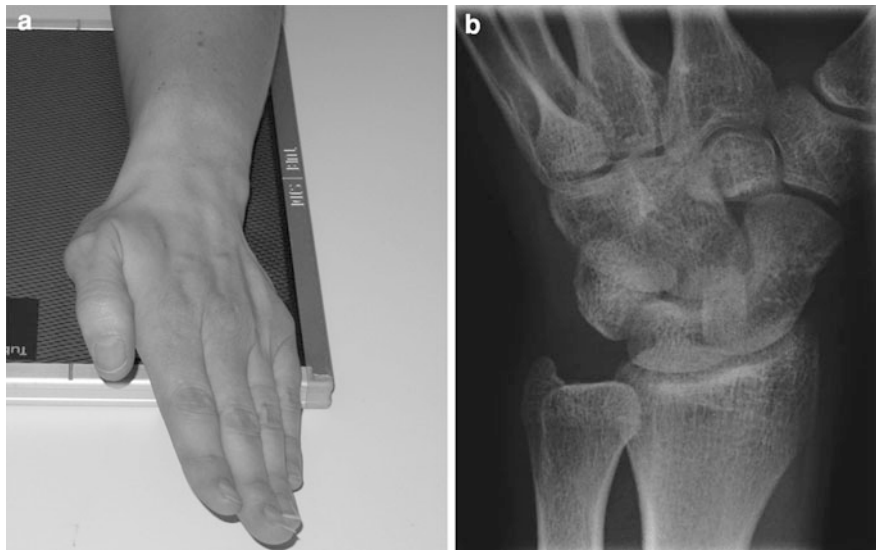

Fig. 8 **a** Patient positioning for anterior oblique of the carpus. **b** Anterior oblique radiograph of the carpus

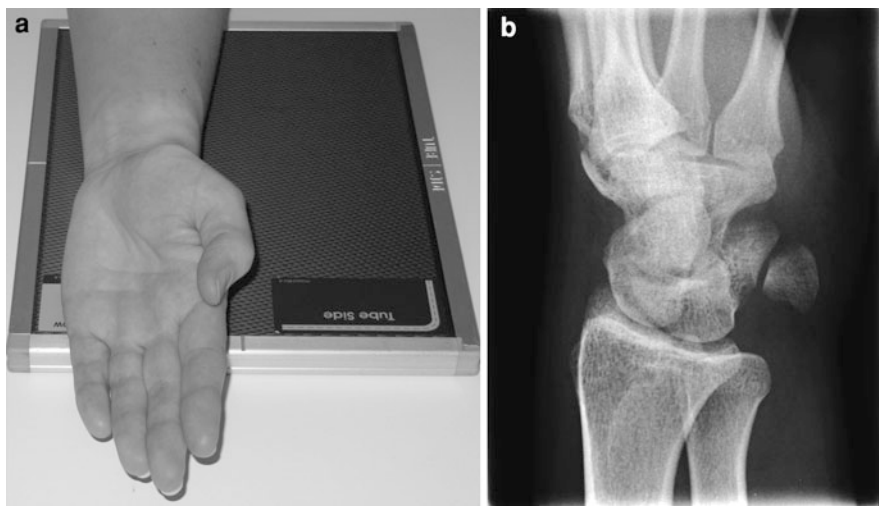

Fig. 9 **a** Patient positioning for posterior oblique of carpus. **b** Posterior oblique radiograph of carpus

Evaluation

The PA hand projection should demonstrate all of the joints of the hand, carpus and wrist (Fig. 11). The joint spaces should be symmetrical and parallel. This projection is used in the evaluation of trauma, arthropathy and a range of miscellaneous conditions. The carpo-metacarpal joint may be evaluated with a line drawn between the distal articular surfaces of the trapezoid, capitate and hamate and the parallel articular surfaces of the second-fifth metacarpals (Fig. 12) (Fisher and Rogers 1983). Discontinuity of this line should raise a suspicion of fracture and or dislocation.

2.3.2 PA Anterior Oblique Hand

Technique

The hand is externally rotated by 45° from the PA projection (Fig. 13). The fingers should be extended and separated. The film is centered over the third metacarpal head.

Fig. 10 Lateral radiograph of carpus

Evaluation

This projection is very useful for evaluating the shafts and necks of the metacarpals (Fig. 13). The phalanges are seen in an oblique plane. The first and second metacarpals are usually separated whilst there is an overlap of the fourth and fifth metacarpals.

2.3.3 Lateral Hand

Technique

The hand is placed in the lateral position on the cassette with the medial border of the wrist and hand resting on the cassette. The fingers are extended. The thumb is also extended and placed clear of the rest of the hand (Fig. 14). The centering point is the head of the second metacarpal.

Evaluation

This projection (Fig. 14) is useful for evaluating the carpal metacarpal region for dislocation. It is helpful in evaluating the fifth metacarpal shaft fractures. This projection is also used for foreign body assessment.

2.3.4 Posterior Oblique of Both Hands

Technique

Both hands are placed on the cassette. They should lie symmetrically. Both forearms are supinated with 45° of rotation. The radial styloid is elevated from the cassette on both sides. The centering point is midway between the hands at the level of the fifth metacarpal head.

Evaluation

The metacarpal heads should all be clearly seen and separated (Fig. 15). The purpose of this projection is to evaluate the metacarpal heads for bone erosion. This projection has also been termed the Norgaard view or 'ball catcher's' view. The obliquity of the projection enables a different part of the metacarpal head to be shown in profile. It is considered that this improves the visualisation of bone erosions from rheumatoid disease as more of the beam is tangential to the bare area of the metacarpal head, the area susceptible to erosions. This is when compared with the conventional PA projection. However, two studies have demonstrated that there is limited additional information with this projection (De Smet and Martin 1981; Edwards and Edwards 1983).

2.4 Radiographic Projections of the Phalanges

The standard projections are PA and lateral. Supplementary oblique views either of individual phalanges or as part of a PA oblique hand examination may also be undertaken. The oblique projection does not substitute for the lateral view which is an essential projection when evaluating trauma.

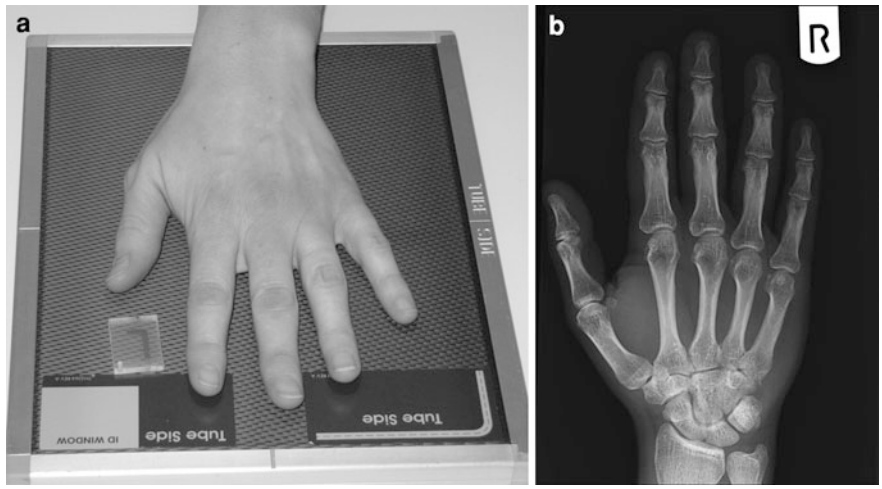

Fig. 11 **a** Patient positioning for PA hand. **b** Radiograph of PA hand

Fig. 12 PA hand radiograph showing level for assessment of parallelism across carpo–metacarpal joint (*white arrow*)

2.4.1 PA Phalanges

Technique

The phalanges may be X-rayed individually or in pairs. For example, the second and third phalanges are imaged together or the fourth and fifth are imaged together. The fingers are placed on the cassette with a hand in the neutral PA position (Fig. 16). The centering is over the PIP joint of the relevant finger. The X-ray should include the distal third of the metacarpal as far as the soft tissue of the fingertip.

Evaluation

The joint spaces should be uniform and parallel (Fig. 16).

2.4.2 Lateral Phalanges

Technique

The phalanges may be X-rayed individually or in pairs. Typically, the second and third are imaged together or the fourth and fifth phalanges. The phalanges are extended and separated so that both are visible on the film. The centering point is the proximal interphalangeal joint of the affected finger (Fig. 17).

Evaluation

The lateral view is especially important in the evaluation of volar plate injuries and extends or extensor avulsion injuries. The phalanx must be X-rayed in the true lateral position (Fig. 17).

2.5 Radiographic Evaluation of the Thumb

The conventional projections of the thumb are AP and lateral. They are performed separately from the examination of the hand. The PA projection may be substituted for the AP projection when there is pain or difficulty in achieving the appropriate position.

2.5.1 AP Thumb

Technique

The forearm is over-pronated such that the thumb lies on the cassette (Fig. 18). The centering point is the base of the first metacarpal.

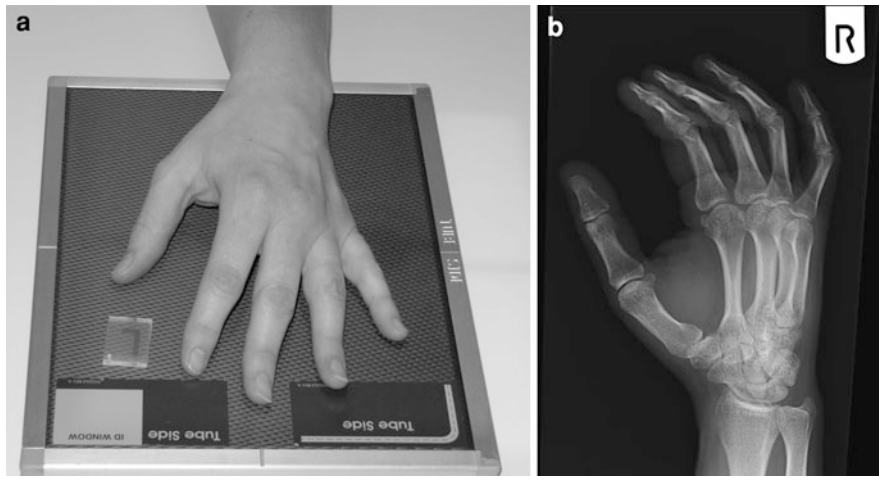

Fig. 13 **a** Patient positioning for PA anterior oblique of hand. **b** Radiograph of PA anterior oblique of hand

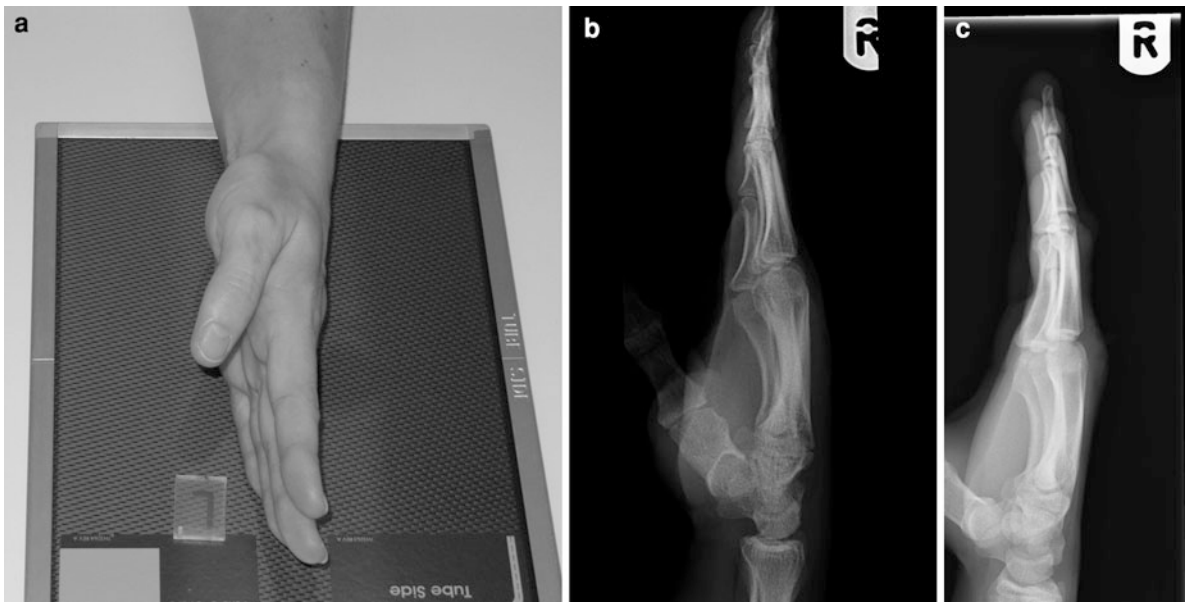

Fig. 14 **a** Patient positioning for lateral radiograph of hand. **b** Lateral radiograph of hand. **c** Soft tissue lateral radiograph of hand

Evaluation

The base of the first metacarpal and the base of the proximal phalanx of the thumb are well demonstrated and can be assessed for fracture (Fig. 18).

2.5.2 Lateral Thumb

Technique

The thumb is rested on the cassette in the lateral position. The palm of the hand is slightly rotated to bring thumb into it through lateral profile. The centering point is the metacarpo–phalangeal joint (Fig. 19).

Evaluation

This projection is important for evaluation of the base of the first metacarpal for fracture (Fig. 19).

2.5.3 PA Thumb

Technique

The medial border of the hand is rested on the cassette. The hand is rotated forwards with the thumb extended until a PA view of the thumb is obtained (Fig. 20). It is important that the thumb is extended, otherwise there is overlap at the metacarpal phalangeal joint. This projection is used when it is not

Fig. 15 Posterior-oblique (ball-catcher's) radiograph of the hands

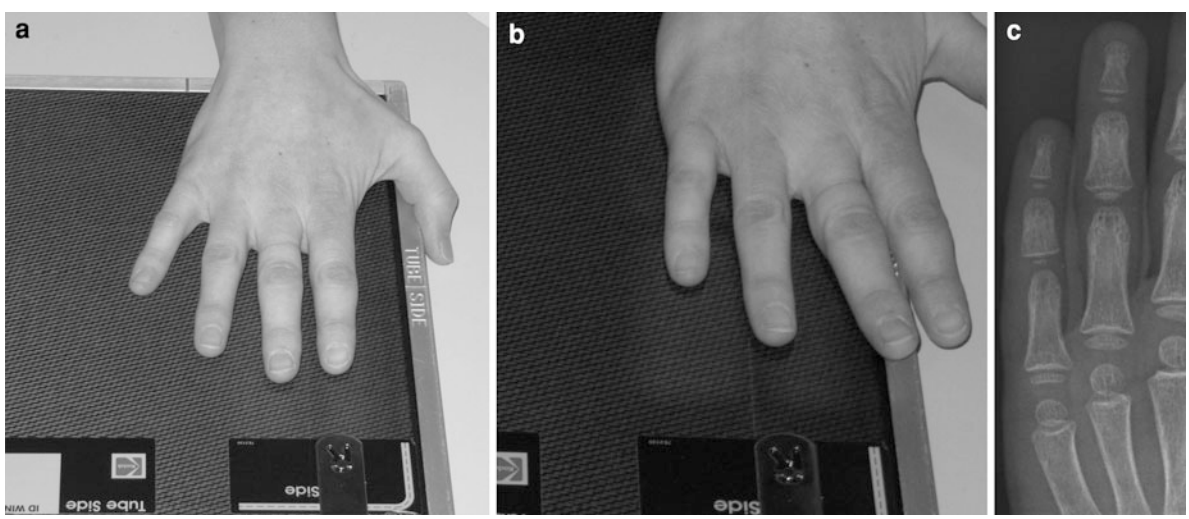

Fig. 16 **a** Patient positioning for PA second and third fingers. **b** Patient positioning for PA fourth and fifth fingers. **c** Radiograph of PA fingers

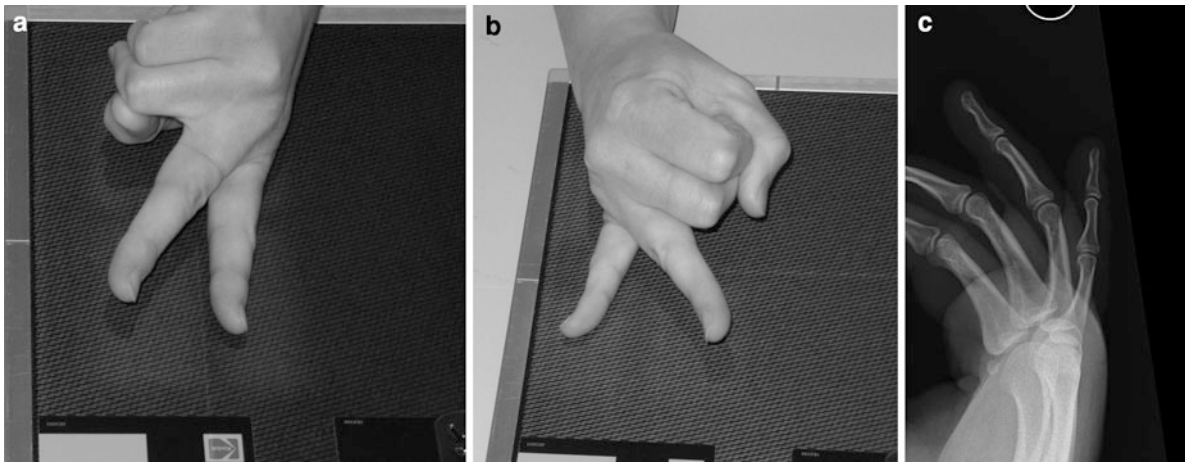

Fig. 17 **a** Patient positioning for lateral of second and third fingers. **b** Patient positioning for lateral of fourth and fifth fingers. **c** Lateral radiograph of fingers

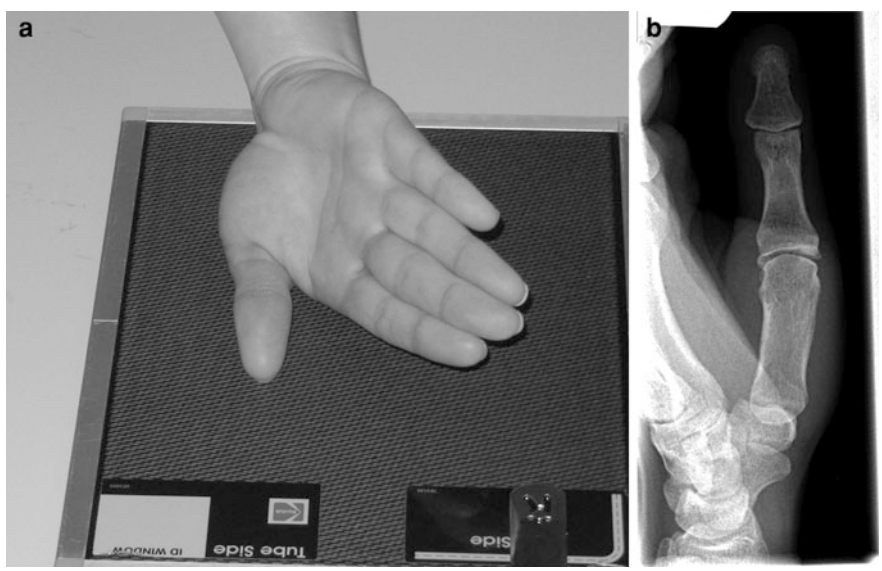

Fig. 18 **a** Patient positioning for AP thumb. **b** AP radiograph of thumb

possible for the patient to achieve the over-pronation of the forearm required for the AP projection.

Evaluation

Care must be taken to obtain a good PA view and to assess for parallelism at the metacarpal–phalangeal joint.

3 Radiographic Technique

Film screen technique has been the standard methodology used for plain film radiographic examination for many years. With the advent of digital radiography and the growth in picture archiving and storage systems, new techniques have been introduced which are replacing standard film screen radiography. Computed radiography (CR) was the first technique, introduced in the 1980s. Direct digital radiography is a more recent technique introduced in the 1990s.

Imaging may be thought of in four separate steps: generation, processing, archiving and presentation. Image generation commences when X-rays having passed through the object under examination reach the detector. In the case of film screen radiography, this will be the film. The interaction of X-ray photons with the film results in a latent image which is then processed to

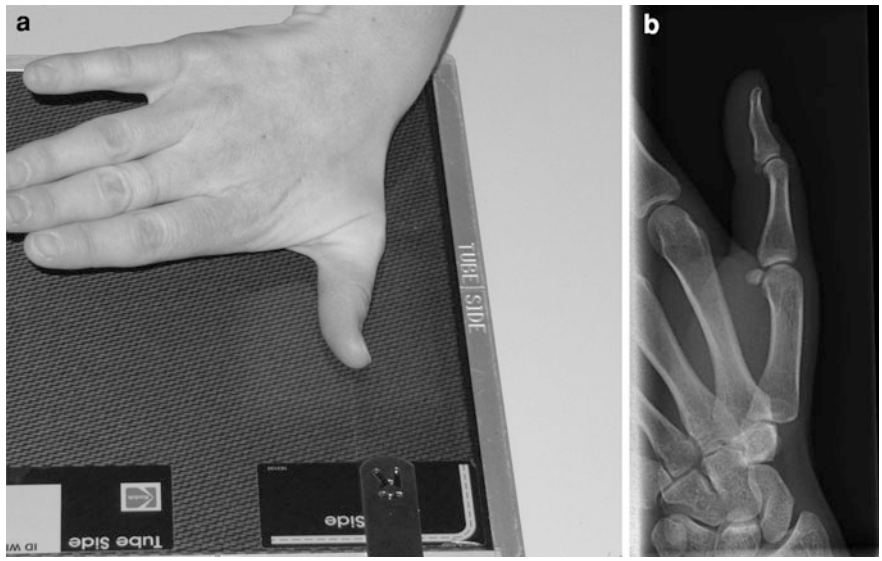

Fig. 19 **a** Patient positioning for lateral thumb. **b** Lateral radiograph of thumb

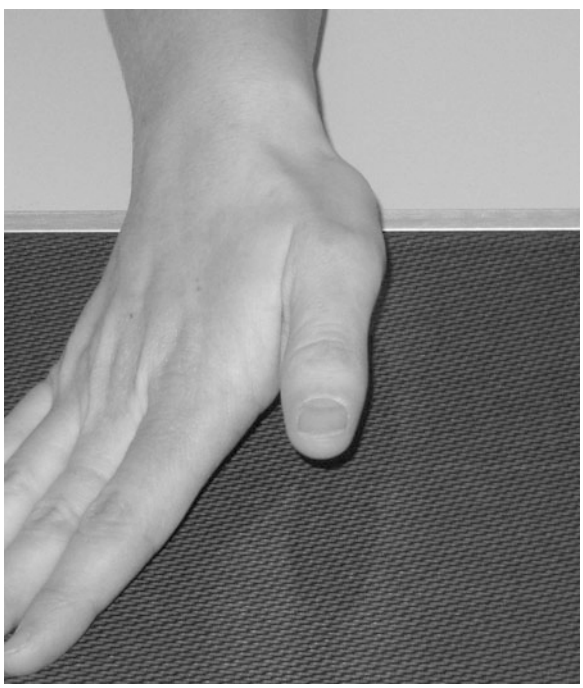

Fig. 20 Patient positioning for PA thumb

produce the real image which is 'stored' on the film. In the case of film-screen radiography, all the four steps are performed on the film. In the case of digital imaging, these steps are separated. CR differs from direct radiography (DR) in the content of these steps. Modern digital imaging produces images of the same quality as conventional film-screen radiography.

3.1 Computed Radiography (CR)

CR uses a cassette-based detector plate comprising photostimulable phosphor. Photons interacting with the phosphor elevate the energy levels of electrons within the phosphor crystals, and this comprises the latent image. The cassette is then taken to a processor. The processor (image plate reader) scans the plate with a helium–neon laser, releasing the energy from the excited electrons. Light is emitted which is converted by photomultiplier tubes into an analog signal which may then be digitised. Specific processing algorithms are then applied to this information resulting in the image for transfer and display. Images are displayed on computers or may be printed out on laser film. The plate is then exposed to intense light to completely erase the latent image and enable a further exposure with the same plate.

The processing algorithms which are used are specific to the body part and the suspected pathology. A key strength of digital imaging is its latitude and ability to display both bone and soft tissue detail with great clarity. It is necessary to optimise the image processing to the body part. Therefore, for example,

the processing algorithm for a hip X-ray will be different to the knee and different again to the hand. Also a soft tissue foreign body film will be processed differently to a skeletal film for a fracture. The raw data may be reprocessed as required. A limitation of CR is that the resolution is of the order of 2.5–5 lines per mm. This contrasts with film screen radiography of 2.5–15 lines per mm. However, 2.5 lines per mm is acceptable for standard skeletal radiography.

Whereas overexposure with film screen radiography produces a black film, the processing of an overexposed CR phosphor plate can result in an image which has a normal appearance. The risk of the overexposure is that the radiographer is less able to make a judgment regarding standard exposures. It is easy for there to be an upward creep in exposure factors over a period of time. Thus, careful quality control mechanisms are required. A useful but imperfect guide is the 'exposure index'. Underexposure results in increasing graininess of the image.

For certain applications, high-resolution CR plates have been produced. In general, they would be limited to paediatric applications but may also be used for detailed extremity skeletal work.

3.2 Direct Radiography (DR)

DR produces high-quality digital images. DR has a major impact upon workflow in the radiology department as the image is produced very quickly after exposure. An image is produced 10–40 s after exposure. This enables a rapid decision with regard to the adequacy of the image (exposure, positioning and collimation). With DR the generation and processing occur in the same device which may be placed in, or replace the standard Bucky tray. DR is based upon solid-state, flat panel, digital radiography detectors. These detectors use a very thin layer of amorphous silicon.

The typical DR detector used in skeletal work uses indirect conversion. The detector comprises a combination of a layer of X-ray fluorescent material and the amorphous silicon active matrix read-out array. X-ray photon energy interacts with thallium-activated caesium iodide releasing light photons which are detected in a 2D array of amorphous silicon diodes. An electronic signal is produced which is then digitised. The caesium thallium is applied onto the hydrogenated amorphous silicon. Each pixel in the active matrix array comprises a light-sensitive element (photodiode) together with an associated switching component. The switching component is either in the form of a thin film diode switch or a thin film transistor switch. The charge pattern resulting from the exposure is read out amplified and digitised.

With both CR and DR, an anti-scatter grid is required. The dynamic range of DR is approaching 10,000:1. As a result of this, DR detectors have wide dose latitude. As with CR, this enables good quality images of both bone and soft tissue. DR also suffers from the potential weakness of incremental exposure drift or 'creep' as described above.

Active development of both DR and CR detectors continues with the aim of further refinements to produce improved quality images. In the case of DR, alternative manufacturing methods for large amorphous silicon active matrix arrays are a subject of research. Improvement in X-ray absorption materials for both CR and DR is an important area of development.

Digital imaging has provided the opportunity for immense workflow improvement and image storage with picture archiving and communications systems (PACS). In many centres, PACS has replaced conventional film imaging. The advantages are numerous. Importantly they include the ability to view images at multiple locations simultaneously; storage and retrieval efficiency; and image manipulation and interrogation. Advanced digital imaging techniques take advantage of the improved processing power leading to the development of tomosynthesis, dual energies subtraction and temporal subtraction imaging.

4 Additional Projections and Fluoroscopy

The radiographic evaluation of carpal instability includes a static series and dynamic fluoroscopy. The objective of these examinations is to demonstrate malalignment of the carpal bones either in a static position or alternatively as part of a dynamic examination. The dynamic examination also provides the opportunity to assess for dysynchronous movement between the carpal bones. Malalignment or dysynchronous movement is likely to be a consequence of ligament disruption. Of particular importance in this regard are the scapholunate and lunotriquetral

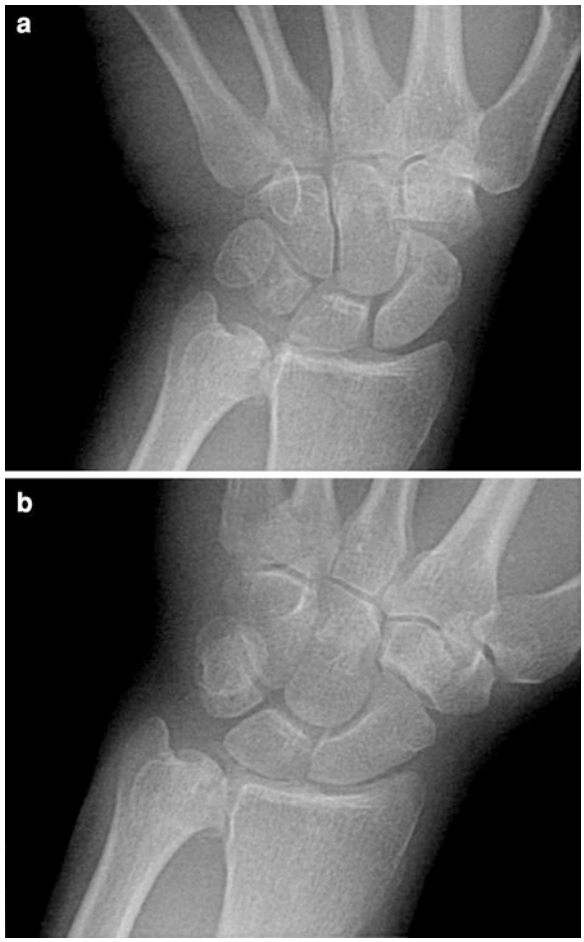

Fig. 21 Fluoroscopy images of PA wrist **a** ulna deviation and **b** radial deviation

ligaments. Both have strong anterior and posterior components with a thin 'membranous' central portion.

4.1 Carpal Instability Series—Static Evaluation

4.1.1 Technique

The standard series would include the following projections (Gilula et al. 1984). Initially, the wrist is placed in the neutral PA position. From this, the wrist is deviated in the ulnar and then radial directions (Fig. 21). Images are taken in all three positions. Following this, this series is repeated with the fist clenched. In some cases, the technique may be conducted with the fist clenched around a pencil or a tennis ball (Schmitt and Froehner 2006). Then three further views are performed with the wrist in the lateral position: neutral, full extension and full flexion (Fig. 22). An additional view which is performed for evaluation of the piso-triquetral joint is the 30° supinated view of the wrist.

4.1.2 Evaluation

The integrity of the carpal arcs is assessed. Congruency of the intercarpal joints and the width of these joints is also assessed. Of particular importance with regard to the proximal carpal row is the relationship of the lunate relative to the radius (Schernberg 1990). The proximal surface of the lunate should not move more than half of its width on the distal surface of the radius (Fig. 21).

4.2 Dynamic Evaluation—Fluoroscopy

4.2.1 Technique

A dynamic study (Gilula et al. 1984; Braunstein and Louis 1985) provides a further opportunity to assess for carpal instability in the situation where the static views are negative. Essentially, the static series are repeated with movement. Therefore, from the PA neutral position the wrist is deviated in the ulnar direction and then back through the neutral position to the radial position. This movement is repeated. From the lateral position the wrist is fully flexed and then fully extended. This is also repeated as required. A further, non-standard part of the study follows enquiry of the patient with regard to the movement causing symptoms. The patient undertakes this movement which is recorded with fluoroscopy. This study may be recorded and therefore replayed at normal and reduced speeds.

4.2.2 Evaluation

The alignment of the carpal bones in all the positions is evaluated. In addition, careful viewing of the relative movements within each carpal row and then between carpal rows is important. For the proximal carpal joint, the movement of the lunate relative to the distal radius is important. For the metacarpal joint, the movement of the hamate relative to the lunate is important.

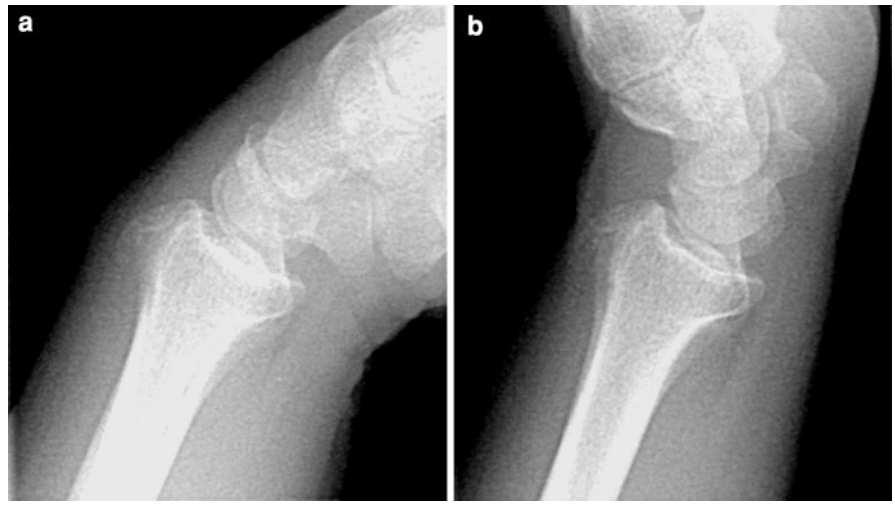

Fig. 22 Fluoroscopy images of lateral wrist in **a** flexion and **b** extension

Fig. 23 Measurement of ulna variance. Solid line is ulna neutral (normal). + is positive ulna variance and – represents negative ulna variance

5 Measurements

There are a number of measurements which are useful in the assessment of the wrist which can be performed on plain radiographs (Mann and Wilson 1992; Goldfarb and Yin 2001; Rosner and Zlatkin 2004; Loredo and Sorge 2005). Ulna variance is useful in a range of conditions including assessment following fracture and ulna-sided wrist pain. Distal radial measurements include radial inclination, radial length, and palmar tilt. These are all useful in the assessment of distal radial fractures. The scapholunate and capitate–lunate angles are calculated when carpal instability is suspected. Finally, carpal height is measured when collapse of the carpus is suspected, for example, as a consequence of carpal instability or previous fracture.

5.1 Ulna Variance

Ulna variance is the difference in length between the distal radius and the distal ulna. This measurement is relevant in a number of carpal disorders including fracture assessment and abnormalities of the proximal carpal row such as chondromalacia of the lunate. The wrist is assessed in a neutral PA position. A technique for the assessment of ulna variance involves first, identifying the long axis of the radius at 2.0 and 5.0 cm from the distal radial cortex. A perpendicular running tangential to the most ulna portion of the distal radial articular cortex is then drawn to this line. Second, the line is drawn tangential to the distal ulna and parallel to the line described above (Mann and Wilson 1992; Loredo and Sorge 2005) (Fig. 23). In negative ulna variance (ulna minus), the ulna is shorter than the radius. In positive ulna variance (ulna plus), the ulna is longer than the radius. Normally, the radius and ulna are of the same length or there is mild negative ulna variance.

Fig. 24 Measurement of radial inclination. Normal inclination is 21–25°

Fig. 25 Measurement of radial length. Normal measurement is 10–13 mm

5.2 Radial Inclination

Radial inclination describes the slope of the radius between the tip of the radial styloid and the ulnar border of the radius in the frontal or PA plane. Its assessment is important following distal radial fractures (Mann and Wilson 1992; Loredo and Sorge 2005). The technique for obtaining the measurement is first to identify the long axis of the radius as described above (Sect. 5.1). Second, a line is drawn from the tip of the radial styloid to the ulnar border of the distal radius. The third line is drawn through the intersection of these lines, perpendicular to the long axis of the radius (Goldfarb and Yin 2001). The radial inclination is the angle between the perpendicular and the line running tangential to the radial styloid and ulnar border of radius (Fig. 24). The normal inclination is 23° (21–25°) (Goldfarb and Yin 2001).

Fig. 26 Measurement of palmar tilt (volar inclination). Normal value 0–22°

5.3 Radial Length (Radial Height)

Radial length (radial height) is a method for assessing shortening of the radius, for example, following a fracture. The measurement involves identification of the

Fig. 27 Scapholunate angle. White lines represent long axis of scaphoid and lunate. Normal range is 30–60°

Fig. 28 Capitolunate angle. White lines represent long axis of lunate and capitate. Normal range is 0–30°

long axis of the radius. Two lines perpendicular to this are then constructed. Firstly, tangential to the tip of the radial styloid and secondly tangential to the ulnar border of the distal radius (Fig. 25). The distance between these two lines is the radial length (Goldfarb and Yin 2001). A normal value of 10–13 mm is expected.

5.4 Palmar Tilt (Volar Tilt or Volar Inclination)

This measurement assesses the tilt of the distal radius at the radiocarpal joint. The central axis of the radius is identified in the lateral plane using points at 2 and 5 cm from the midpoint of the distal articular surface. A perpendicular is drawn to this line at the articular surface. A third line is drawn from the dorsal lip of the distal radius to the volar lip of the distal radius. The palmar tilt is the angle between the third line and the perpendicular (Fig. 26). It is normally between 0–22° (Mann and Wilson 1992; Goldfarb and Yin 2001). This is an important measurement in the assessment of distal radial fractures.

5.5 Scapholunate Angle

This angle is calculated when carpal instability is suspected (Goldfarb and Yin 2001). It is particularly pertinent in the assessment of dorsal intercalated instability (DISI). The angle is measured from the lateral view of the wrist. The angle is calculated by drawing two lines (Timins and Jahnke 1995). A line is drawn through the proximal and distal volar convexities of the scaphoid. This defines the scaphoid axis. The lunate axis is perpendicular to a line drawn between the distal poles of the lunate. The normal scapholunate angle lies between 30–60° (Fig. 27).

5.6 Capitate–Lunate Angle

This angle is calculated when the volar instability pattern (VISI) of carpal instability is suspected. The angle is measured from the lateral view of the wrist. The long axis of the lunate is drawn as described above (Sect. 5.5). The long axis of the capitate is drawn from the centre of its distal articular surface to the centre of the proximal articular surface (Timins and Jahnke 1995). The normal capitate–lunate angle lies between 0 and 30° (Fig. 28).

5.7 Carpal height

Carpal height provides quantification of the degree of carpal collapse e.g. in scapholunate advanced collapse

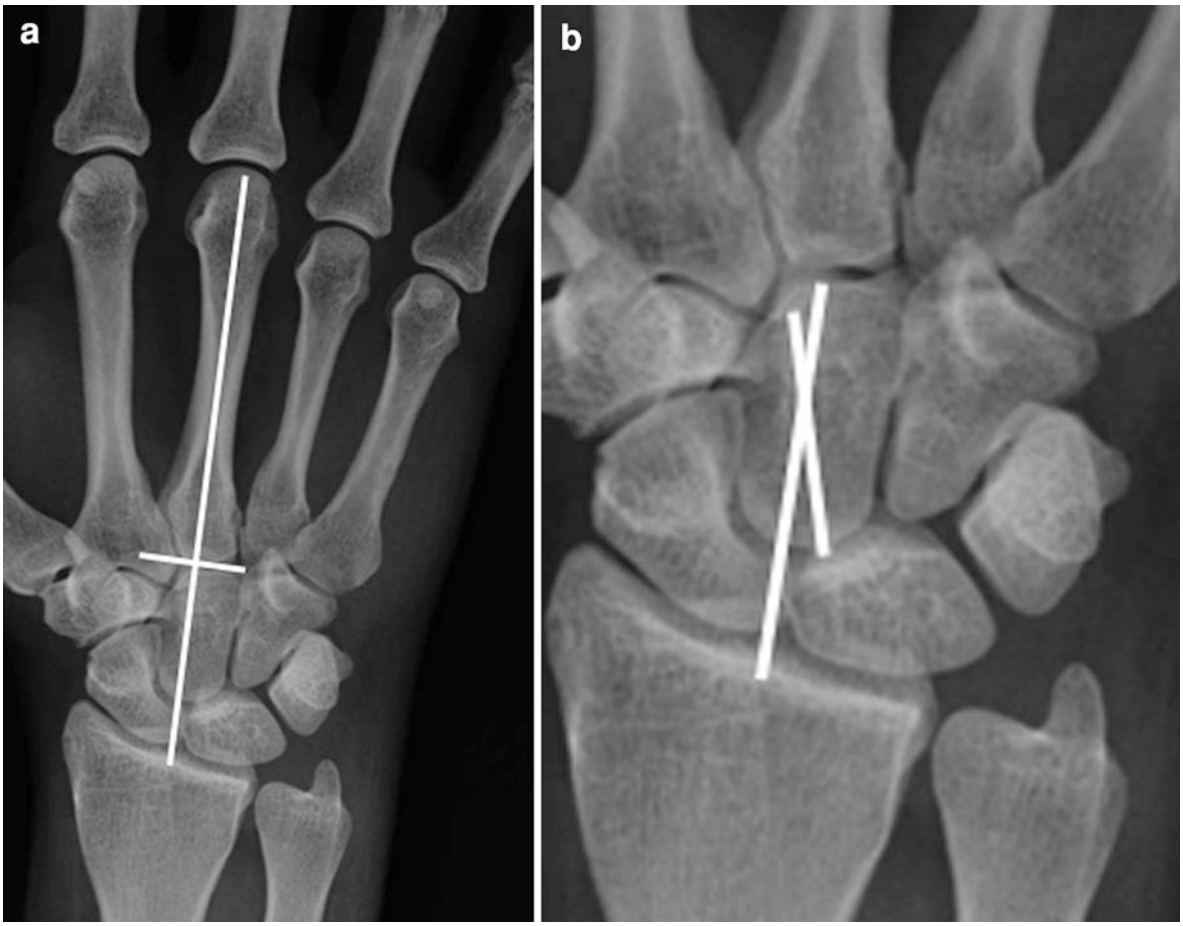

Fig. 29 Measurement of carpal height **a** method 1 and **b** method 2

(SLAC). Two methods have been described. The first method describes a ratio between the distance from the base of the third metacarpal to the proximal articular surface of the radius and the length of the third metacarpal. The line drawn extends from the long axis of the third metacarpal (Fig. 29a). With this method, the normal carpal height ratio is 0.54 (Mann and Wilson 1992).

The second method divides the carpal height (distance from base of the third metacarpal to proximal articular surface of radius) by the capitate length. The capitate length is calculated from the distal angular articular surface of the capitate (between the bases of the second and third metacarpals) and the centre of the proximal articular surface of the capitate (Fig. 29). The normal figure is 1.57 (Mann and Wilson 1992).

A carpal height index is obtained by dividing the carpal height of the diseased wrist with the normal wrist (Loredo and Sorge 2005). This index may be followed with time as a marker of disease progression.

6 Arthrography

Arthrography of the wrist is performed in the assessment of interosseous wrist ligaments and the triangular fibrocartilage complex. Specifically, it is performed for assessment of the scapholunate and luno-triquetral ligaments in addition to the triangular fibrocartilage complex. With the advent of cross-sectional imaging techniques, it is most frequently undertaken now as part of an MRI or CT arthrographic study. The basic technique is that of a proximal row or radiocarpal injection. A more complex study will involve injection of two or three wrist compartments.

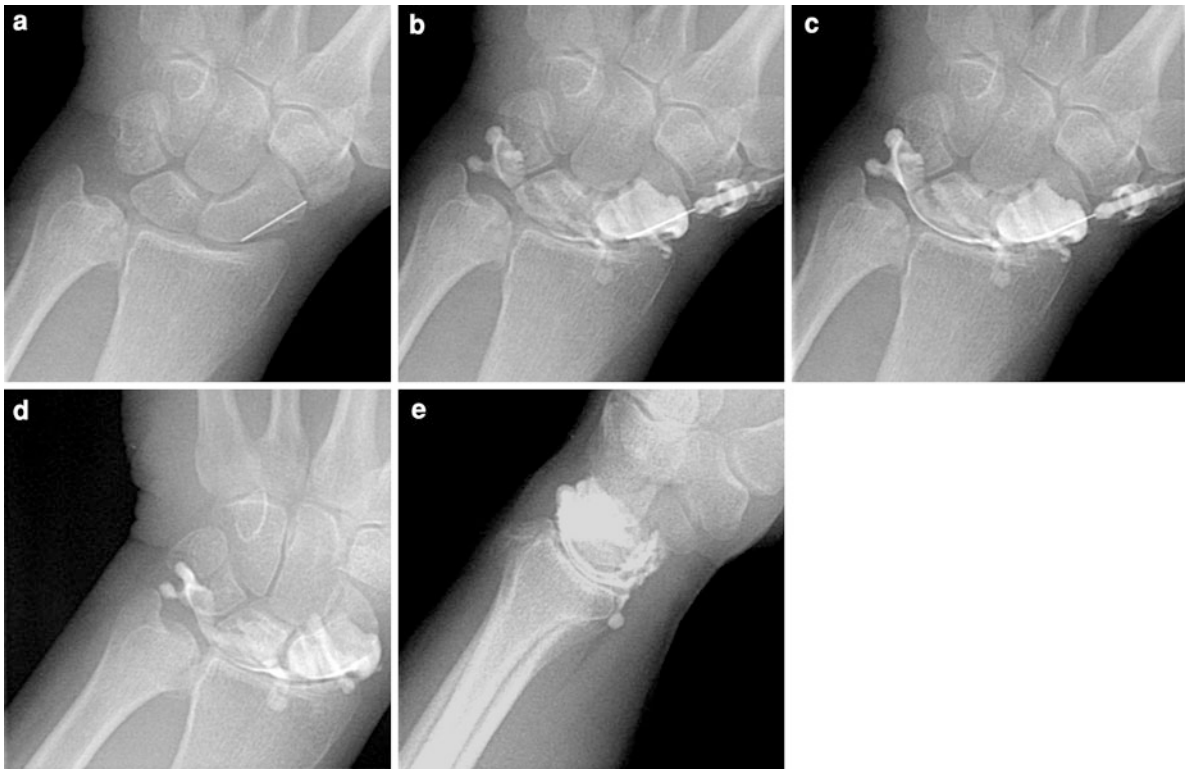

Fig. 30 Fluoroscopy images from radiocarpal arthrogram **a** needle position **b** early filling with contrast **c** mid-filling phase **d** late-filling phase (complete) **e** lateral view post exercise

Unicompartmental injection to the radiocarpal (Fransson 1993) may be undertaken by injection at two different points. The first is a dorsal approach to the junction between the scaphoid and lunate just proximal to the scapholunate ligament. The second is between the scaphoid and distal radius. The wrist is gently flexed and a 22G needle introduced under fluoroscopic guidance. Care must be taken not to damage the scapholunate ligament. Note should be taken of the normal radial inclination and allowance made for the dorsal lip of the radius when introducing the needle.

Contrast is injected into the radiocarpal space. The usual filling volume is between 2 and 4 ml. The end of the injection is signified by gentle resistance to further filling and distribution of contrast across the radiocarpal joint. Generally, contrast of 240 IU/l is sufficient for good radiographic imaging. The mixture injected will alter for CT arthrography and MRI arthrography as is described in subsequent chapters.

Contrast should be injected slowly, carefully observing the filling of the radiocarpal space and looking for contrast tracking into the scapholunate space, lunate triquetral space, or distal radio–ulnar joint. Spot films are taken during injection (Fig. 30). At the end of the injection when there is good filling of the radiocarpal space, a further series of films is taken following gentle exercise of the wrist. A typical series of films would include PA in the neutral, ulnar deviation, and radial deviation positions followed by a lateral view. It is commonplace to have performed a static and dynamic instability series (as outlined earlier in the chapter) prior to injection of contrast.

Fluoroscopy and videotaping the procedure enabled further retrospective analysis (Gilula and Totty 1983).

The normal pattern of filling (Fig. 30) outlines the radiocarpal joint (Resnick 1995). Age-related degenerate perforations of the central portion of the scapholunate and lunate triquetral ligaments are well recognized (Linkous and Pierce 2000). Similarly age-related degenerate perforations of the radial side of the triangular fibrocartilage complex with filling of the distal radio-ulnar joint may also be observed. Small volar outpouchings (radial recesses) of the capsule are well recognized (Fig. 30). On the ulnar

Fig. 31 Fluoroscopy image from midcarpal arthrogram demonstrating needle position and filling of radiocarpal space

side there is a small pre-styloid recess above which the meniscus homologue and a further collection of contrast may be identified. Filling of the piso-triquetral space is a normal variant.

Midcarpal injection has been described by Tirman and Weber (1985). The wrist is gently flexed. The midcarpal joint is injected between the distal scaphoid and capitate (Linkous and Pierce 2000) (Fig. 31). Careful injection with fluoroscopic guidance is undertaken until good filling of the space has been obtained. Careful observation of the scapholunate and lunotriquetral spaces is undertaken, looking for evidence of filling of these spaces. Tirman regarded this as an easier method for establishing the integrity of the scapholunate and lunotriquetral ligaments. A static and dynamic instability series would be obtained.

Triple compartment arthrography (Levinsohn and Palmer 1987; Levinsohn and Rosen 1991) was introduced by Levisnohn and regarded as being of superior diagnostic quality. However, Steinbach and Palmer (2002) preferred single joint injection into the radiocarpal space. This has the advantage of single as opposed to multiple injections, whilst still providing the opportunity to evaluate the scapholunate ligament, lunotriquetral ligament, and triangular fibrocartilage complex. It also avoids the time-consuming wait between each of the three compartment injections whilst awaiting absorption of contrast.

However, the diagnostic yield is greater with a midcarpal injection based on an analysis of unidirectional joint communications (Wilson and Gilula 1991). It was proposed that if a scapholunate or lunotriquetral ligament disruption was suspected then a midcarpal injection should be performed first. If a triangular fibrocartilage complex disruption was suspected, then a radiocarpal injection should be performed first.

Full triple compartment arthrography also involves injecting the distal radio–ulnar joint looking for communication with the proximal carpal joint.

Digital subtraction imaging was introduced to improve visualisation of scapholunate or lunotriquetral space filling when multiple compartments were injected (Quinn and Pittman 1988) without the normal three-hour delay between injections waiting for the contrast to be absorbed.

In current radiological practice, the arthrogram is usually performed in conjunction with an MRI arthrogram or CT arthrogram. Whilst 3T MR without arthrography is producing very high-quality images of the wrist (Saupe 2009) and its associated ligaments, MRI arthrography is preferred for evaluation of the ligamentous structures of the wrist (Magee 2009; Sofka and Pavlov 2009).

References

Braunstein EM, Louis DS (1985) Fluoroscopic and arthrographic evaluation of carpal instability. AJR Am J Roentgenol 144(6):1259–1262

De Smet AA, Martin NL (1981) Radiographic projections for the diagnosis of arthritis of the hands and wrists. Radiology 139(3):577–581

Edwards JC, Edwards SE (1983) The value of radiography in the management of rheumatoid arthritis. Clin Radiol 34(4):413–416

Fisher MR, Rogers LF (1983) Systematic approach to identifying fourth and fifth carpometacarpal joint dislocations. AJR Am J Roentgenol 140(2):319–324

Fransson SG (1993) Wrist arthrography. Acta Radiol 34(2):111–116

Gilula LA (1979) Carpal injuries: analytic approach and case exercises. AJR Am J Roentgenol 133(3):503–517

Gilula LA, Totty WG (1983) Wrist arthrography. The value of fluoroscopic spot viewing. Radiology 146(2):555–556

Gilula LA, Destouet JM et al (1984) Roentgenographic diagnosis of the painful wrist. Clin Orthop Relat Res 187:52–64

Goldfarb CA, Yin Y (2001) Wrist fractures: what the clinician wants to know. Radiology 219(1):11–28

Levinsohn EM, Palmer AK (1987) Wrist arthrography: the value of the three compartment injection technique. Skeletal Radiol 16(7):539–544

Levinsohn EM, Rosen ID (1991) Wrist arthrography: value of the three-compartment injection method. Radiology 179(1):231–239

Linkous MD, Pierce SD (2000) Scapholunate ligamentous communicating defects in symptomatic and asymptomatic wrists: characteristics 1. Radiology 216(3):846–850

Loredo RA, Sorge DG (2005) Radiographic evaluation of the wrist: a vanishing art. Semin Roentgenol 40(3):248–289

Magee T (2009) Comparison of 3-T MRI and arthroscopy of intrinsic wrist ligament and TFCC tears. AJR Am J Roentgenol 192(1):80–85

Mann FA, Wilson AJ (1992) Radiographic evaluation of the wrist: what does the hand surgeon want to know? Radiology 184(1):15–24

Quinn SF, Pittman CC (1988) Digital subtraction wrist arthrography: evaluation of the multiple-compartment technique. AJR Am J Roentgenol 151(6):1173–1174

Resnick D (ed) (1995) Diagnosis of bone and joint disorders. W.B. Saunders, Philadelphia

Resnik CS (2000) Wrist and hand injuries. Semin Musculoskelet Radiol 4(2):193–204

Rosner JL, Zlatkin MB (2004) Imaging of athletic wrist and hand injuries. Semin Musculoskelet Radiol 8(1):57–79

Saupe N (2009) 3-Tesla high-resolution MR imaging of the wrist. Semin Musculoskelet Radiol 13(1):29–38

Schernberg F (1990) Roentgenographic examination of the wrist: a systematic study of the normal, lax and injured wrist. Part 1: the standard and positional views. J Hand Surg Br 15(2):210–219

Schmitt R, Froehner S (2006) Carpal instability. Eur Radiol 16(10):2161–2178

Sofka CM, Pavlov H (2009) The history of clinical musculoskeletal radiology. Radiol Clin North Am 47(3):349–356

Steinbach LS, Palmer WE (2002) Special focus session. Radiographics 22(5):1223–1246

Timins ME, Jahnke JP (1995) MR imaging of the major carpal stabilizing ligaments: normal anatomy and clinical examples. Radiographics 15(3):575–587

Tirman RM, Weber ER (1985) Midcarpal wrist arthrography for detection of tears of the scapholunate and lunotriquetral ligaments. AJR Am J Roentgenol 144(1):107–108

Whitley AS (2005) Clark's positioning in radiography. Hodder Arnold, London

Wilson AJ, Gilula LA (1991) Unidirectional joint communications in wrist arthrography: an evaluation of 250 cases. AJR Am J Roentgenol 157(1):105–109

Yang Z, Mann FA (1997) Scaphopisocapitate alignment: criterion to establish a neutral lateral view of the wrist. Radiology 205(3):865–869